Article

Leveraging the Activated Monomer Mechanism to Create Grafted Polymer Networks in Epoxide–Acrylate Hybrid Photopolymerizations

Brian F. Dillman, Sage M. Schissel and Julie L. P. Jessop *

Department of Chemical & Biochemical Engineering, The University of Iowa, Iowa City, IA 52242, USA
* Correspondence: jessop@che.msstate.edu; Tel.: +1-662-325-2480

Abstract: Hybrid epoxide–acrylate photopolymerization enables the temporal structuring of polymer networks for advanced material properties. The ability to design polymer network architectures and to tune mechanical properties can be realized through the control of the cationic active center propagation reaction (active chain end mechanism) relative to the cationic chain transfer reaction (activated monomer mechanism). Grafted polymer networks (GPNs) can be developed through the covalent bonding of epoxide chains to acrylate chains through hydroxyl substituents, making hydroxyl-containing acrylates a promising class of chain transfer agents. This work demonstrates the formation of these GPNs and explores the physical properties obtained through the control of hydroxyl content and hybrid formulation composition. The GPNs exhibit a lower glass transition temperature than the neat epoxide network and result in a more homogeneous network. Further investigations of hydroxyl-containing acrylates as chain transfer agents will generate a wider range of physical property options for photopolymerized hybrid coatings, sealants, and adhesives.

Keywords: cationic ring-opening photopolymerization; free-radical photopolymerization; hydroxyl group; dynamic mechanical analysis; gel permeation chromatography

1. Introduction

Hybrid photopolymerization affords opportunities to structure polymer networks in time and to engineer advanced material properties [1]. Using light to initiate polymerization rather than heat enables significant savings in energy costs, processing space, and time; solvent-free systems; and increased control over the production of initiating species [2–5]. Acrylates and cycloaliphatic epoxides are common monomers used in the industrial photopolymerizations of coatings, adhesives, and sealants. The extensive selection of acrylate monomers offers many options for polymer physical property development. In epoxide systems, the activated monomer (AM) mechanism provides a pathway toward improving kinetics and tuning polymer properties [6–8]. The selection of acrylate monomers that promote the AM mechanism has the potential to create grafted polymer networks with an enhanced control of the kinetics, physical properties, phase separation, and network stability in photopolymerized epoxide–acrylate hybrid systems [9–12].

In these epoxide–acrylate hybrid systems, the epoxide moiety undergoes cationic ring-opening photopolymerization, while the acrylate moiety undergoes free-radical photopolymerization. Free-radical chain polymerization is most commonly used in current photopolymer industries for its quick cure time and easily modified monomers and oligomers [2,13]. However, free-radical polymerization is subject to oxygen inhibition, shrinkage, and shrinkage stress [13–16]. In contrast, cationic chain polymerization is relatively slow and affected by moisture [17]. However, it is not inhibited by oxygen and results in little or no shrinkage.

In addition, the cationic active centers persist for long times, enabling dark and shadow cures [18,19].

Through the combination of these two independent reactive systems, hybrid epoxide–acrylate polymers exhibit lower sensitivity to oxygen and moisture and offer advantages such as an increased cure speed and improved film-forming properties [20,21]. For example, acrylate coatings exhibit surface tackiness due to oxygen diffusion at the air-monomer interface. However, in the hybrid system, cationic polymerization becomes the dominant route of conversion at the sample surface, resulting in tack-free coatings [20]. These hybrid systems also show promise in abating free-radical polymerization-induced shrinkage by adjusting the epoxide–acrylate ratio [22]. The ability to sequence the two independent reactions with a large selection of available monomers also allows for greater control over property tuning in a hybrid system. Careful control of the independent reactions in a hybrid system is required; otherwise, the first reaction can limit the second through vitrification or topological restraint and thus affect monomer conversion [23].

Another opportunity to develop physical properties in hybrid systems is the formation and alteration of polymer networks [2,4]. In interpenetrating networks (IPNs), distinct polymer systems are joined only through co-entanglement. When each network is independently cross-linked, a full-IPN results (Figure 1) [24]. A semi-IPN is the entanglement of a cross-linked polymer network and a linear polymer. The cross-link density of IPNs can affect polymer properties as well as phase separation (the formation of homopolymer domains caused by a lack of mutual solubility) [25]. The cross-link density of each polymer can be controlled by adding chain transfer agents and/or altering the functionality of the monomer [23,26–28].
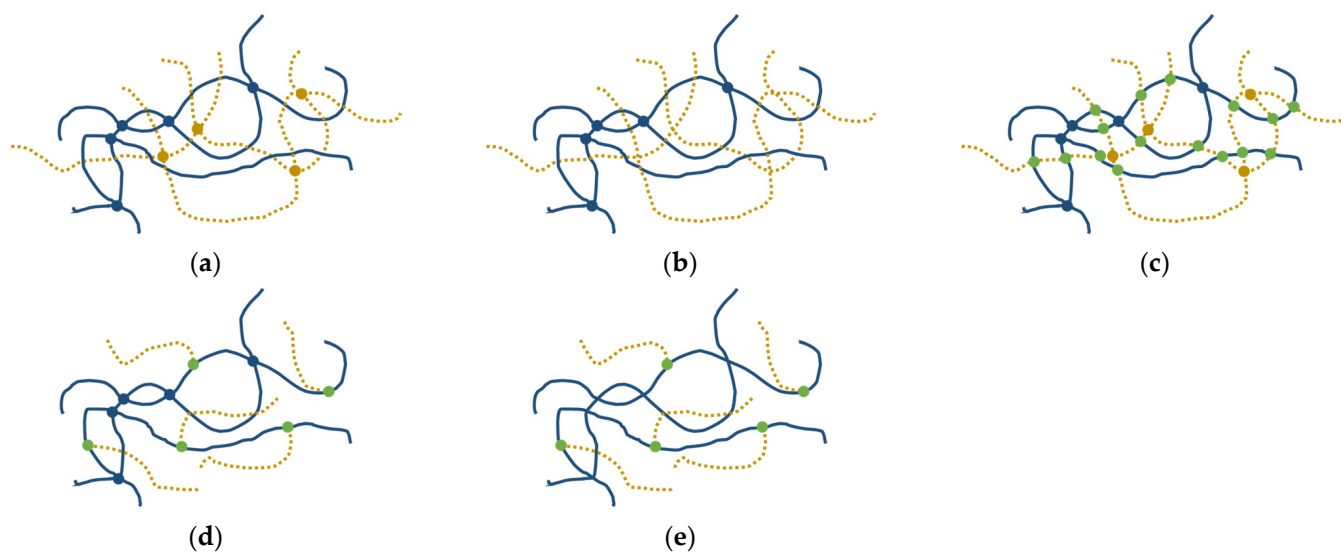
Figure 1. Network structures formed from hybrid polymerizations—Polymer 1 is a solid navy line, Polymer 2 is a dashed gold line, and covalent bonds between polymer chains are solid dots (navy for 1-1, gold for 2-2, and green for 1-2): (**a**) full interpenetrating network (IPN), Polymers 1 and 2 are cross-linked; (**b**) semi-IPN, Polymer 1 is cross-linked, Polymer 2 is linear; (**c**) full grafted polymer network (GPN), Polymers 1 and 2 are cross-linked and grafting occurs; (**d**) semi-GPN, Polymer 1 is cross-linked, linear Polymer 2 is grafted to Polymer 1; (**e**) graft polymer, linear Polymer 2 is grafted to linear Polymer 1. Adapted from Reference [24].

Hybrid formulations can also be designed to create grafted polymer networks (GPNs). GPNs form when the two polymers are not only co-entangled but are also covalently bonded together. Covalent bonds between polymers are achieved through the presence of a secondary functional group on one monomer, which is able to react with the second monomer. Hybrid monomers, such as 3,4-epoxy-cyclohexyl-methyl methacrylate (METHB),

contain both an epoxide and an acrylate moiety to provide the link between the two polymer systems formed in an epoxide–acrylate hybrid polymerization [20].

However, the unique attributes of the cationic polymerization provide an opportunity to form GPNs and reduce phase separation in cationic/free-radical hybrid systems without the addition of a hybrid monomer. Cationic active centers can form a polymer chain through either the active chain end (ACE) mechanism or the activated monomer (AM) mechanism [6,10,29,30]. The ACE mechanism is a propagation reaction in the traditional sense in that the polymer chain grows through the addition of a monomer to the cationic active center at one end. The AM mechanism is a chain transfer reaction in which water or an organic alcohol reacts with the cationic active center, capping the growing chain with a hydroxyl group and releasing a proton that can start a new polymer chain. For example, including hydroxyl-containing acrylates in the hybrid formulation facilitates the AM mechanism for an epoxide and results in the covalent bonding of the epoxide polymer system to the acrylate polymer system [9–12,31–33]. Controlling the dominance of one mechanism with respect to the other provides an effective means to tune GPN properties based on the concentrations of epoxide and hydroxyl groups and the reactivity of the cationic active centers.

Thus, hydroxyl-containing acrylates could comprise a promising class of chain transfer agents (CTAs). Polyols based on ethers such as tetrahydrofuran (THF) and propylene glycol are common CTAs used in epoxide formulations for coatings, adhesives, and sealants. With the oxygen in the backbone, these polyols provide flexibility, but are less stable for applications requiring long-term durability [34,35]. Polyacrylates, on the other hand, possess better hydrolytic stability, and provide more opportunities to tune the physical properties of the polymer network with a wider selection of monomer structures. In addition, as long as some hydroxyl-containing acrylate is included in the hybrid formulation, the covalent bonding between the epoxide and acrylate chains could prevent the phase separation seen in IPNs [25], resulting in a high stability of the network's physical properties.

In this work, GPNs were demonstrated by grafting epoxide polymer chains onto hydroxylated acrylate polymer chains through the AM mechanism. The extent of AM propagation vs. ACE propagation was investigated via gel permeation chromatography (GPC) of grafted polyacrylates that varied in the degree of hydroxylation. The polyacrylates were also formulated in cross-linking resins to determine their effectiveness as CTAs in formulations containing epoxides.

2. Materials and Methods

2.1. Materials

Sodium hydride (60% dispersion in mineral oil), carbon disulfide, 1-dodecanethiol, and chloroacetonitrile were purchased from Acros Organics (Waltham, MA, USA). Cyclohexene oxide (CHO), butyl acrylate (BA), chloroform-d (the solvent used for ^{1}H NMR spectroscopic analysis), polyTHF 250 (average M_n~250), diethyl ether, and azobisisobutyronitrile (AIBN) were purchased from Sigma Aldrich (Burlington, MA, USA). 4-Hydroxybutyl acrylate (HBA) was donated by BASF (Florham Park, NJ, USA). PC-2506 (diaryliodonium cationic photoinitiator) and PC-1000 (diepoxide monomer) were donated by Polyset Company (Mechanicville, NY, USA). Monomers and CTAs are shown in Figure 2. All materials were used as received.
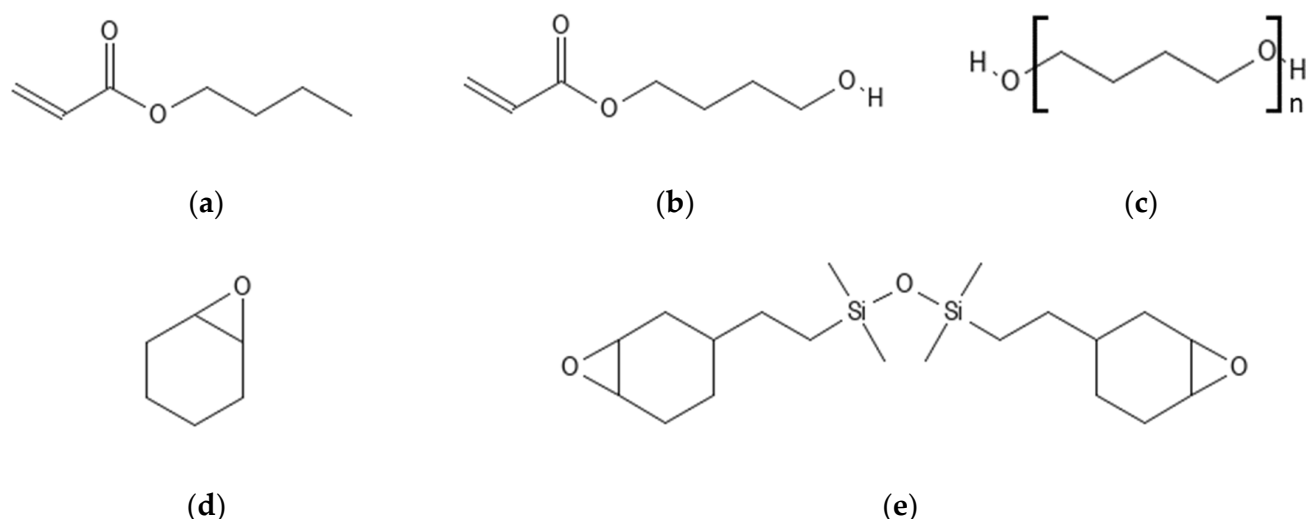
Figure 2. Chemical structures: (**a**) butyl acrylate (BA), (**b**) 4-hydroxybutyl acrylate (HBA), (**c**) polyTHF 250, (**d**) cyclohexene oxide (CHO), and (**e**) PC-1000 (diepoxide monomer).

2.1.1. RAFT Agent Synthesis

The chain transfer agent (RAFT agent), cyanomethyl dodecyl trithiocarbonate, was synthesized according to published methods in order to produce polyacrylates via reversible addition–fragmentation chain-transfer (RAFT) polymerization, which is a controlled radical polymerization method [36–38]. Sodium hydride (1.723 g, 43.08 mmol) was placed in a three-neck flask. The mineral oil was extracted from sodium hydride by washing with three 10 mL portions of hexane via syringe under nitrogen. The three-neck flask was placed in an ice bath and fitted with a pressure-equalizing addition funnel containing 1-dodecanethiol (7.7083 g, 38.1 mmol), diluted with diethyl ether (20 mL), which was added over a period of 10 min. A bright yellow precipitate was observed and stirred for 30 min. Carbon disulfide (3.1129 g, 40.9 mmol) was then added through the addition funnel. A bright green precipitate was formed and then filtered to obtain sodium trithiocarbonate. Chloroacetonitrile (1.2389 g, 16.4 mmol) was added to the trithiocarbonate/diethyl ether slurry and stirred for approximately 3 h. The yellow solution was dried over anhydrous sodium sulfate. The solvent was then removed via rotary evaporation, and yellow oil was obtained. Upon cooling to room temperature, the product (RAFT agent) formed a waxy solid. NMR spectra of the product were collected using an AVANCE 300 MHz spectrometer (Bruker, Billerica, MA, USA), confirming an approximate yield of 55%.

2.1.2. RAFT Polymer Synthesis

Two polyacrylates were synthesized via RAFT polymerization in order to produce polymers with a dispersity close to 1 (Figure 3). The first was neat poly(butyl acrylate) (poly(BA)). BA (12.1485 g, 94.8 mmol), RAFT agent (0.4006 g, 1.3 mmol), and the free-radical initiator AIBN (0.0223 g, 0.1 mmol) were added to a 50 mL round-bottom flask and stirred until dissolved. The contents were purged with nitrogen for 5 min and then plunged into a 65 °C water bath for 2 h. After 2 h, the solution was opened to the air and cooled with an ice bath to quench the reaction. The same procedure was used to prepare the second acrylate polymer: poly(butyl acrylate-ran-4-hydroxy butyl acrylate) (poly(BA-ran-HBA)), in which BA and HBA were in a 10:1 molar ratio. Here, BA (10.9463 g, 85.4 mmol), HBA (1.3844 g, 9.6 mmol), RAFT agent (0.4006 g, 1.3 mmol), and AIBN (0.0207 g, 0.1 mmol) were stirred in a 50 mL round-bottom flask and polymerized.

(**a**) (**b**)
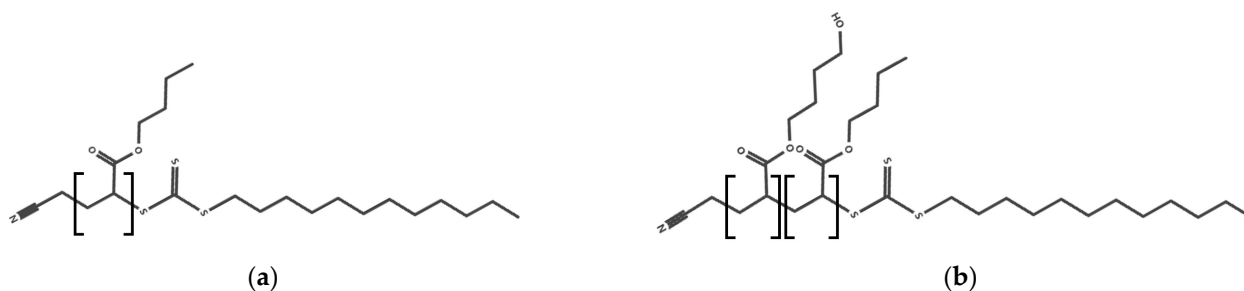
Figure 3. Molecular structure of the polyacrylates formed via RAFT polymerization: (**a**) homopolymer, poly(BA), and (**b**) the random copolymer, poly(BA-ran-HBA), containing 90 mol% BA and 10 mol% HBA.

The solutions gelled, and NMR spectroscopy confirmed that very high conversions were obtained (>90%). The polymer was poured into a cold methanol/water (70:30) mixture (500 mL), the liquid was decanted, and the polymer product was allowed to degas for about 3 days. Following this procedure, no unreacted monomer was detected via NMR spectroscopy. Gel permeation chromatography (GPC) confirmed that the dispersities of poly(BA) and poly(BA-ran-HBA) were 1.04 and 1.03, respectively.

2.1.3. Linear Epoxide Thermal Polymerization

Linear polyethers were synthesized through the thermal polymerization of CHO in order to demonstrate grafting on the epoxide through the AM mechanism. Thermal conditions were chosen over photocuring conditions due to the volatility of CHO. The cationic photoinitiator (PI) was still used since it can also serve as a thermal initiator [39]; however, higher PI concentrations are needed in this scenario. CHO was polymerized using 7 wt% PI under three conditions (Table 1): neat (Figure 4) and in the presence of each of the two polyacrylates. The three mixtures were heated in a water bath at 70 °C under reflux for 24 h. After polymerization, the solvent was removed via rotary evaporation, and the polymers were analyzed via GPC.

Table 1. Linear epoxide (CHO) formulations for GPC samples.

Formulation	CHO, g	Cationic PI, g	Polyacrylate, g	CHCl$_3$, mL
Neat epoxide	5.033	0.378	–	10
Epoxide + poly(BA) (10:1)	5.050	0.374	0.516	10
Epoxide + poly(BA-ran-HBA) (10:1)	5.051	0.370	0.500	10
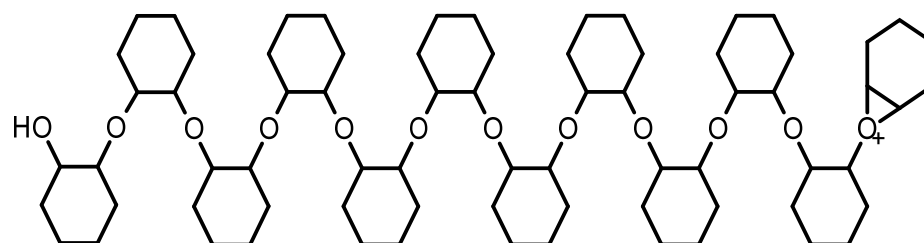
Figure 4. Molecular structure of the linear polyether formed through the ACE propagation of CHO.

2.1.4. Cross-Linked Epoxide Photopolymerization

Cross-linked polyethers were synthesized through the photopolymerization of the diepoxide monomer in order to establish changes in physical properties due to grafting through the AM mechanism. The diepoxide monomer was photopolymerized using 3.5 wt% of the cationic photoinitiator under multiple conditions (Table 2). In addition to the formulations containing the polyacrylates, formulations containing varying amounts of

polyTHF 250 (a chain transfer agent studied previously [6]) were prepared for comparative purposes. After mixing, each formulation was placed in glass molds prepared from silanized (Rain-X® treated) glass slides, which were separated by a double thickness of 150 μm glass cover slips. The molds were placed under a low irradiance (~2–5 mW/cm^2) black light, which emits a band of wavelengths centered around 365 nm, for 5 min per side. Then, each resin-filled glass mold was passed, twice on each side, through a belt-driven curing system (model LC-6B, Fusion, Gaithersburg, MD, USA), which was fixed with an irradiator (model 1300 MB) comprised of an aluminum reflector and a high-intensity Hg lamp (H-bulb). The belt speed was 9 ft/min (0.05 m/s), delivering a UV exposure of ~3.5 J/cm^2 per run. The samples were placed in an oven at 150 °C for 2 h. This annealing procedure ensured that no additional epoxide polymerization occurred during the dynamic mechanical analysis [40,41]. The resulting polymers were cooled to room temperature before DMA testing.

Table 2. Cross-linked diepoxide formulations for DMA samples.

Formulation	Diepoxide, g	Cationic PI, g	Polyacrylate. g	PolyTHF 250, g
Neat epoxide	5.002	0.195	–	–
Epoxide + poly(BA) (10:3)	5.002	0.193	1.489	–
Epoxide + poly(BA-ran-HBA) (10:3)	5.016	0.193	1.507	–
Epoxide + polyTHF (10:0.7)	5.008	0.189	–	0.330
Epoxide + polyTHF (10:1.5)	5.009	0.190	–	0.814
Epoxide + polyTHF (10:3)	5.023	0.189	–	1.629

2.2. Analytical Methods

2.2.1. Gel Permeation Chromatography

GPC using chloroform as the mobile phase (1.0 mL/min) was performed at room temperature. A Waters 515 HPLC pump was used for the GPC (DAWN HELEOS II, Wayatt Technology, Santa Barbara, CA, USA). Four Waters columns (styragel HR2, HR4, HR4, and HR6) were used in series. Polystyrene standards with molecular weights of 4950 g/mol; 10,850 g/mol; and 28,500 g/mol were diluted with chloroform to concentrations of approximately 1 g/L. Chromatograms of the standards were collected using a refractive index detector (RID), and elution times were identified as follows: 14.1 min for 28,500 g/mol, 16.0 min for 10,850 g/mol, and 18.3 min for 4950 g/mol. The resulting calibration curve, with an R^2 value of 0.9843, was as follows:

$$\log M = -0.1787t + 6.9438 \tag{1}$$

where *M* is the polymer molecular weight, and *t* is the elution time in minutes. Five different linear polymer samples were diluted to approximately 10 g/L with chloroform and analyzed via GPC to determine elution times: neat poly(BA), neat poly(BA-ran-HBA), neat CHO, CHO + poly(BA), and CHO + poly(BA-ran-HBA).

2.2.2. Dynamic Mechanical Analysis

Specimens for dynamic mechanical analysis (DMA) were prepared from the synthesized cross-linked polymers. The polymers were removed from the glass molds, and specimens were cut to approximate dimensions of 15 mm × 5 mm × 0.3 mm. A Q800 dynamic mechanical analyzer (TA Instruments, New Castle, DE, USA) was used to characterize the thermo-mechanical properties of the polymer specimens. Samples were placed in a vertical film tension clamp and ramped from −100 to 250 °C at a heating rate of 3 °C/min and with a 1 Hz sinusoidal strain of 0.05%. The glass transition temperature (T$_g$) was taken as the temperature corresponding to the tan δ maximum. Data were smoothed using a 7-point moving average.

3. Results and Discussion

3.1. Demonstration of Grafting

In order to determine if the AM mechanism could promote grafting between epoxide and acrylate polymer chains, three different linear polymers were formed and analyzed independently via GPC, along with combinations thereof. The linear poly(cyclohexene oxide) (poly(CHO)) was the product of thermally-initiated cationic polymerization (Figure 4). The two other linear polymers were polyacrylates synthesized via RAFT polymerization: poly(BA) and poly(BA-ran-HBA). Subsequent to RAFT polymerization, these polyacrylates were end-capped with parts of the RAFT agent used to synthesize the materials (see Figure 3). GPC traces (Figure 5) show that both poly(BA) and poly(BA-ran-HBA) have a narrow distribution centered around an elution time of 15.2 min (estimated MW of 16,900 g/mol, Equation (1)). Based on the 10:1 formulation ratio of BA to HBA and the estimated MW for the random copolymer, it is expected that each copolymer chain will have ~12 pendant hydroxyl groups. The molecular weight of the RAFT-synthesized polymers could only increase if the polymers were heated above ~60 °C in the presence of acrylate monomer; however, all excess monomer was removed after the initial synthesis. Poly(CHO) resulted in a broad distribution asymmetrically centered around an elution time of ~17 min (estimated MW of 8050 g/mol, Equation (1)). The distribution associated with poly(CHO) is presumed to be largely formed from the ACE propagation since no chain transfer agent was introduced to the system.
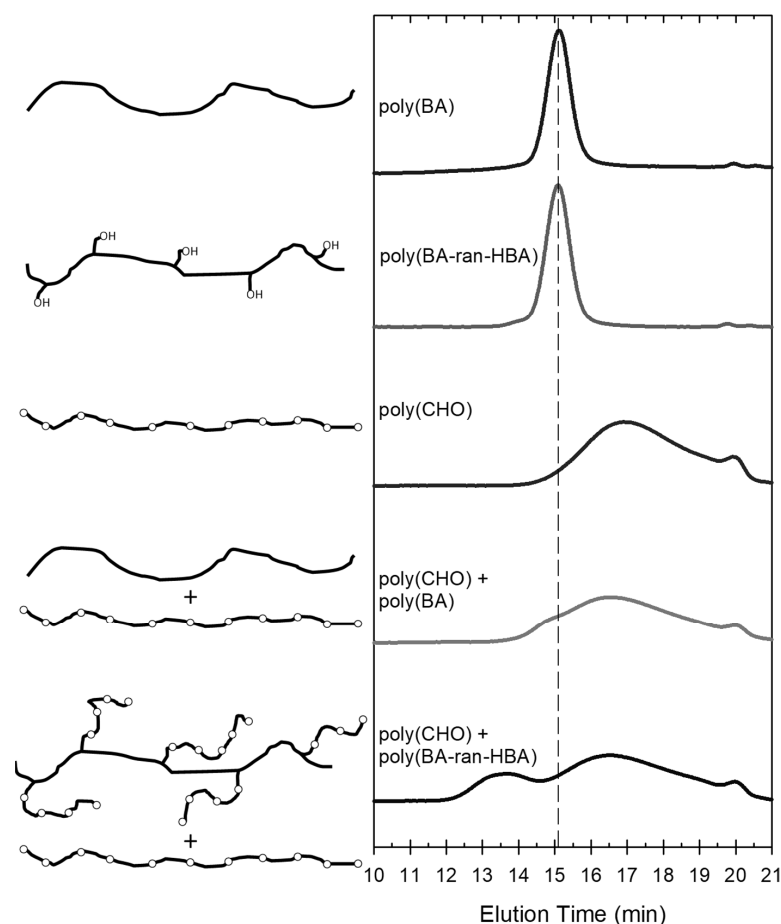

Figure 5. GPC traces of linear polyacrylates (poly(BA) and poly(BA-ran-HBA)), linear polyethers (poly(CHO)), polymer blends (poly(CHO) + poly(BA)), and grafted polymers (poly(CHO) + poly(BA-ran-HBA)). CHO was polymerized in the presence of the polyacrylates rather than simply mixing the polymer products. In the depictions of the polymers on the left, solid lines denote polyacrylates, and solid lines broken by unfilled circles denote polyethers.

According to the AM mechanism, the hydroxyl groups on the poly(BA-ran-HBA) copolymer may react with protonated epoxide monomers during the polyether synthesis. The reaction of the HBA hydroxyl groups with epoxide monomers results in a ring-opening event that regenerates a hydroxyl group. This hydroxyl group may react with another protonated monomer, resulting in graft propagation. The experiments wherein the epoxide monomer was polymerized in the presence of the different polyacrylates demonstrate this process. When polymerized in the presence of poly(BA), the GPC trace of the product shows a similar broad elution distribution to that for neat poly(CHO) with the addition of a small shoulder around the same elution time as the original poly(BA) (15.2 min). The small shoulder indicates that the poly(BA) was indeed inert since no changes in molecular weight were observed. Alternatively, when the epoxide was polymerized in the presence of poly(BA-ran-HBA), a bimodal distribution with a new peak centered around 13.5 min (estimated MW of 34,000 g/mol, Equation (1)) was observed. The decrease in elution time for this peak indicates an increase in molecular weight from the original poly(BA-ran-HBA) material. There is no noticeable shoulder at 15.2 min, indicating that all of the poly(BA-ran-HBA) has been grafted to some extent. The broad distribution associated with the neat cyclohexene oxide polymerization and the ACE mechanism remains, which indicates that the two reaction mechanisms occur in parallel. The polymeric hydroxyl groups promote the AM mechanism, but not to the exclusion of the ACE mechanism.

3.2. GPN Physical Properties

The GPC data show that the acrylate copolymers are incorporated into a graft polymer with the epoxide, thus confirming that the hydroxyl-containing acrylate can function as a CTA. However, the impact of the hydroxyl-containing acrylate on the network properties is not readily apparent since the hydroxyl functionality of the acrylate copolymers is much greater than two and the hydroxyl groups are located along the length of the polymer backbone. Previous work has shown that diols photopolymerized with the industrially relevant diepoxide 3,4-epoxycyclohexylmethyl-3′,4′-epoxycyclohexane carboxylate (EEC) impact the height of the rubbery storage modulus, the magnitude of the T_g, and the width and height of the tan δ peak [6]. To serve as a baseline linking these previous studies to this current work with hydroxyl-containing copolymers, DMA data are presented for the siloxane-containing diepoxide of this study with polyTHF 250 as an additive (Figure 6). The T_g of the diepoxide is ~190 °C, measured after two temperature cycles in the DMA. Since the T_g of polyTHF 250 is subambient, it was not possible to form films stable enough to collect DMA data using the protocol of this study. However, a T_g is reported for polyTHF of −80 °C [42]. This diol was previously shown to effectively modulate the polymer properties of the EEC [6]. Since both the ACE and AM mechanisms take place in these formulations, covalent bonds are formed between the diepoxide and polyTHF 250. These formulations exhibit similar physical properties to those observed in the previous study: each time the concentration of polyTHF 250 doubles, the tan δ peak height doubles, and the T_g decreases by roughly 50 °C. The rubbery modulus, which is proportional to the cross-link density [43,44], also decreases with an increasing polyTHF 250 concentration, spanning an order of magnitude difference between the neat diepoxide and the 10:3 formulation. In addition, increasing the proportion of polyTHF 250 in the formulation results in a much narrower tan δ peak, indicating a more homogeneous network.
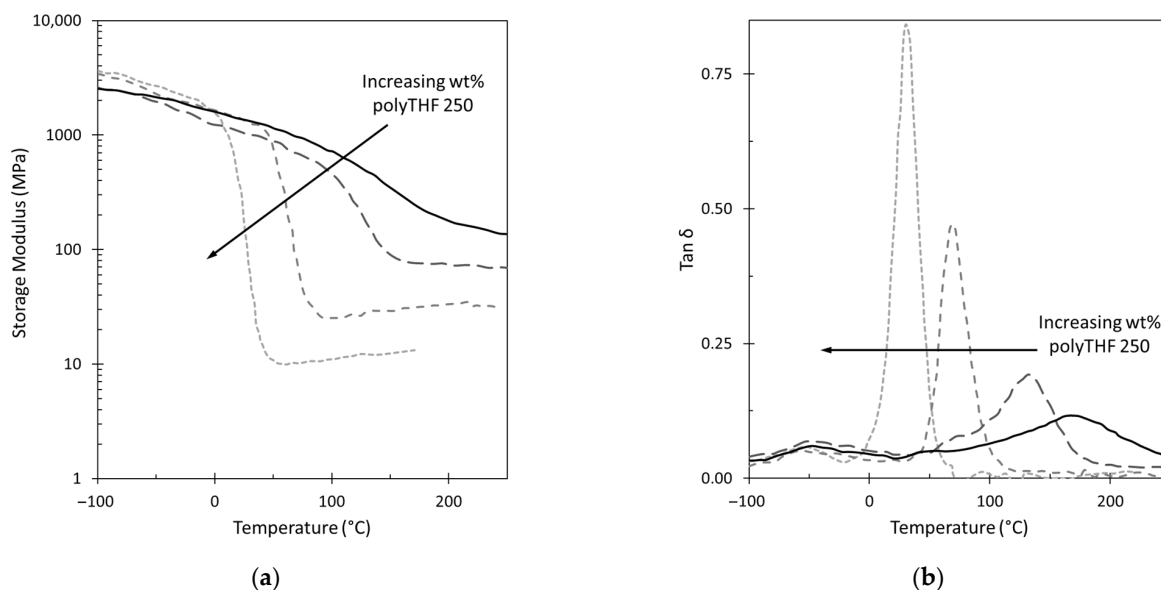
Figure 6. DMA traces showing the storage modulus (**a**) and the tan delta (**b**) for formulations of diepoxide monomer and polyTHF 250. The epoxide + polyTHF 250 composition was equal to 10:0 (black, solid line), 10:0.7 (dark grey, large dash), 10:1.5 (medium grey, medium dash), and 10:3 (light grey, small dash) of the epoxide monomer mass. Polymer specimens were annealed before measurements.

With confirmation that the network properties of the current diepoxide behaved as expected when a diol was introduced to the formulation, an investigation of the grafting of epoxide and acrylate copolymer chains upon network properties proceeded. Polymer networks formed from the cross-linking epoxide resin and the linear polyacrylates were characterized using DMA after annealing the films (Figure 7). As with polyTHF 250, the T_g of the polyacrylates is subambient: the literature value for poly(BA) is −54 °C [45], and that for poly(HBA) is ~−40 °C [46]. Thus, the estimated T_g of the poly(BA-ran-HBA) is ~−53 °C, according to the Fox equation [47].
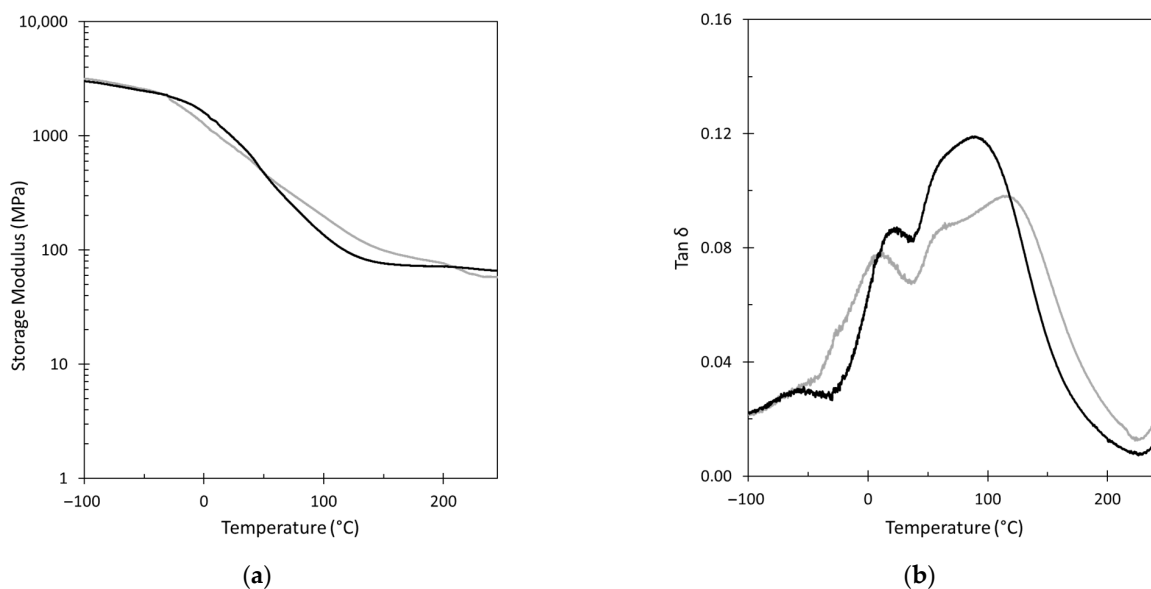
Figure 7. DMA traces showing the storage modulus (**a**) and the tan δ (**b**) for the formulations of diepoxide with poly(BA) (grey line) or poly(BA-ran-HBA) (black line). The epoxide + polyacrylate composition was equal to 10:3. Polymer specimens were annealed before measurements.

For formulations containing the diepoxide and poly(BA), a semi-IPN will be formed since the ACE mechanism is predominant (Figure 1b). However, for formulations containing diepoxide and poly(BA-ran-HBA), a semi-GPN will be formed since there are multiple hydroxyl sites on each polyacrylate through which chain transfer (via the AM mechanism) can occur (Figure 1d). For these covalently bonded networks, a narrower tan δ peak is expected (indicating less phase separation). The DMA data support this visualization of the polymer networks: the material containing the random copolymer yields a narrower glass transition region (greater than a 25% reduction in full-width at half the maximum of the tan δ peak) and a lower T_g than the material containing poly(BA) (~30 °C lower for the peak associated with the predominantly diepoxide network).

Although the findings for the formulation containing the random copolymer are consistent with the general trends observed in epoxide formulations containing CTAs [6], the decrease in T_g and narrowing of the tan δ peak are less pronounced than in formulations containing polyTHF 250. In addition, the height of the tan δ peak, which is related to the damping characteristics of the polymer, is similar for both the material containing the random copolymer and for the neat epoxide material (i.e., both are ~0.12); whereas, at a comparable composition (10:3), the material containing polyTHF 250 has a tan δ over seven times higher than that of the neat epoxide. Moreover, the rubbery modulus of material containing the random copolymer is on the same order of magnitude as the neat epoxide. In the previous study, larger diols were shown to affect the physical properties (T_g, cross-link density, and damping abilities) of the parent resin less drastically than smaller mono-ols [6]. Low-molecular weight, low-functionality CTAs promote a great deal of chain transfer reactions, which delays vitrification, increases the active center mobility, and decreases the ultimate cross-link density. However, high-molecular weight CTAs affect polymer properties less than low-molecular weight CTAs and behave more like a polymer blend or a semi-IPN. Since poly(BA-ran-HBA) has a much higher molecular weight (i.e., ~17,000 g/mol) and functionality than polyTHF 250, the semi-GPN retains the flexibility and damping characteristics of the neat epoxide. To effect larger changes in the physical properties of the semi-GPN, a much higher ratio of acrylate to hydroxyl-containing acrylate may be needed. In addition, there is the opportunity to choose other acrylates or acrylated oligomers to pair with the hydroxyl-containing acrylate to obtain a broader range of physical properties.

4. Conclusions

A trithiocarbonate-type RAFT agent was synthesized and used to produce narrow-molecular weight acrylate polymers, poly(BA) and poly(BA-ran-HBA). During the thermal cationic polymerization of cyclohexene oxide, poly(BA) was inert; however, poly(BA-ran-HBA) facilitated the grafting of epoxide monomers through the AM mechanism. GPC analysis confirmed the grafting and also showed that the AM and ACE mechanisms occurred in parallel.

Formulations of the diepoxide with polyTHF 250 were photopolymerized to benchmark with previous CTA studies. The polyTHF 250 concentration had a large impact on the resulting polymer T_g and cross-linking density, providing further opportunities to tune polymer network properties. When cross-linked polymers were formed from diepoxide resins containing the polyacrylates, only small differences in mechanical behavior were observed between formulations with poly(BA) or poly(BA-ran-HBA). Both polyacrylates reduced the T_g of the material in comparison to the neat diepoxide resin; however, less phase separation was observed with poly(BA-ran-HBA). The similarities in the physical properties of the two systems suggest that the resulting semi-IPNs and semi-GPNs may be comparable.

The random copolymer follows the general trends observed in epoxide formulations containing traditional CTAs; thus, lowering the hydroxyl content of the copolymer may result in realizing the full range of property control. Future work is planned to characterize more fully the GPN-forming systems, including altering the grafting density in the semi-

GPN, testing the effects of uncontrolled acrylate polymerization on polymer properties, and determining the benefits of grafting vs. mixing over time and under end-use conditions. These more in-depth explorations of hydroxyl-containing acrylates as chain transfer agents could provide a wider range of physical property options for photopolymerized hybrid coatings, sealants, and adhesives.

Author Contributions: Conceptualization, B.F.D. and J.L.P.J.; methodology, B.F.D. and J.L.P.J.; formal analysis, B.F.D.; investigation, B.F.D. and S.M.S.; resources, J.L.P.J.; writing—original draft preparation, B.F.D.; writing—review and editing, B.F.D., S.M.S. and J.L.P.J.; visualization, B.F.D. and J.L.P.J.; supervision, J.L.P.J.; funding acquisition, J.L.P.J. All authors have read and agreed to the published version of the manuscript.

Institutional Review Board Statement: Not applicable.

Data Availability Statement: Data are contained within the article.

Conflicts of Interest: The authors declare no conflicts of interest. The funders had no role in the design of the study; in the collection, analyses, or interpretation of data; in the writing of the manuscript; or in the decision to publish the results.

References

1. Oxman, J.D.; Jacobs, D.W.; Trom, M.C.; Sipani, V.; Ficek, B.; Scranton, A.B. Evaluation of initiator systems for controlled and sequentially curable free-radical/cationic hybrid photopolymerizations. *J. Polym. Sci. A Polym. Chem.* **2005**, *43*, 1747–1756. [CrossRef]
2. Odian, G. *Principles of Polymerization*, 4th ed.; John Wiley and Sons, Inc.: Hoboken, NJ, USA, 2004.
3. Salim, M.S. Overview of UV curable coatings. In *Radiation Curing of Polymers II*; Randell, D.R., Ed.; The Royal Society of Cambridge: Cambridge, UK, 1991; pp. 3–21.
4. Fouassier, J. *Photoinitiation, Photopolymerization, and Photocuring: Fundamentals and Applications*; Hanser/Gardner Publication Inc.: Cincinnati, OH, USA, 1995.
5. Pappas, S.P. Radiation curing—A personal perspective. In *Radiation Curing: Science and Technology*; Pappas, S.P., Ed.; Plenum Press: New York, NY, USA, 1992; pp. 1–20.
6. Dillman, B.; Jessop, J.L.P. Chain transfer agents in cationic photopolymerization of a bis-cycloaliphatic epoxide monomer: Kinetic and physical property effects. *J. Polym. Sci. A Polym. Chem.* **2013**, *51*, 2058–2067. [CrossRef]
7. Crivello, J.V.; Liu, S. Photoinitiated cationic polymerization of epoxy alcohol monomers. *J. Polym. Sci. A Polym. Chem.* **2000**, *38*, 389–401. [CrossRef]
8. Biedron, T.; Kubisa, P.; Szymanski, R.; Penczek, S. Kinetics of polymerization by activated monomer mechanism. *Makromol. Chem. Macromol. Symp.* **1990**, *32*, 155–168. [CrossRef]
9. Dillman, B.F. The Kinetics and Physical Properties of Epoxides, Acrylates, and Hybrid Epoxy-Acrylate Photopolymerization Systems. Ph.D. Thesis, University of Iowa, Iowa City, IA, USA, 2013.
10. Schissel, S.M.; Jessop, J.L.P. Enhancing epoxide kinetics and tuning polymer properties using hydroxyl-containing (meth) acrylates in hybrid photopolymerizations. *Polymer* **2019**, *161*, 78–91. [CrossRef]
11. Ajiboye, G.; Jessop, J.L.P. Synergistic effect of hydroxyl-containing acrylates in epoxide acrylate hybrid photopolymerizations. In Proceedings of the 2012 RadTech UV&EB Technology & Conference, Chicago, IL, USA, 30 April–2 May 2012; Available online: https://www.radtech.org/proceedings/2012/papers/Session%209%20-%20Chemistry/GAjiboye_UIowa.pdf (accessed on 7 March 2023).
12. Ge, X.; Ye, Q.; Song, L.; Misra, A.; Spencer, P. Visible-light initiated free-radical/cationic ring-opening hybrid photopolymerization of methacrylate/epoxy: Polymerization kinetics, crosslinking structure, and dynamic mechanical properties. *Macromol. Chem. Phys.* **2015**, *216*, 856–872. [CrossRef] [PubMed]
13. Decker, C. Photoinitiated crosslinking polymerization. *Prog. Polym. Sci.* **1996**, *21*, 593–650. [CrossRef]
14. Davidson, C.L.; Feilzer, A.J. Polymerization shrinkage and polymerization shrinkage stress in polymer-based restoratives. *J. Dentistry* **1997**, *25*, 435–440. [CrossRef] [PubMed]
15. Anseth, K.S.; Bowman, C.N.; Peppas, N.A. Polymerization kinetics and volume relaxation behavior of photopolymerized multifunctional monomers producing highly crosslinked networks. *J. Polym. Sci. A Polym. Chem.* **1994**, *32*, 139–147. [CrossRef]
16. Andrzejewska, E. Photopolymerization kinetics of multifunctional monomers. *Prog. Polym. Sci.* **2001**, *26*, 605–665. [CrossRef]

17. Rajaraman, S.S.K.; Mowers, W.A.; Crivello, J.V. Interaction of epoxy and vinyl ethers during photoinitiated cationic polymerization. *J. Polym. Sci. A Polym. Chem.* **1999**, *37*, 4007–4018. [CrossRef]

18. Nelson, E.W.; Jacobs, J.L.; Scranton, A.B.; Anseth, K.S.; Bowman, C.N. Photo-differential scanning calorimetry studies of cationic polymerizations of divinyl ethers. *Polymer* **1995**, *36*, 4651–4656. [CrossRef]

19. Hoppe, C.C.; Ficek, B.A.; Eom, H.S.; Scranton, A.B. Cationic photopolymerization of epoxides containing carbon black nanoparticles. *Polymer* **2010**, *51*, 6151–6160. [CrossRef]

20. Cai, Y.; Jessop, J.L.P. Decreased oxygen inhibition in photopolymerized acrylate/epoxide hybrid polymer coatings as demonstrated by Raman spectroscopy. *Polymer* **2006**, *47*, 6560–6566. [CrossRef]

21. Cai, Y.; Jessop, J.L.P. Effect of water concentration on photopolymerized acrylate/epoxide hybrid polymer coatings as demonstrated by Raman spectroscopy. *Polymer* **2009**, *50*, 5406–5413. [CrossRef]

22. Sangermano, M.; Carbonaro, W.; Malucelli, G.; Priola, A. UV-cured interpenetrating acrylic-epoxy polymer networks: Preparation and characterization. *Macromol. Mat. Eng.* **2008**, *293*, 515–520. [CrossRef]

23. Dean, K.; Cook, W.D. Effect of curing sequence on the photopolymerization and thermal curing kinetics of dimethacrylate/epoxy interpenetrating polymer networks. *Macromolecules* **2002**, *35*, 7942–7954. [CrossRef]

24. Sperling, L.H. Interpenetrating polymer networks: An overview. In *Advances in Chemistry*; Sperling, L.H., Klempner, D., Utracki, L.A., Eds.; American Chemical Society: Washington, DC, USA, 1994; Volume 239, pp. 3–38. [CrossRef]

25. Hasa, E.; Scholte, J.P.; Jessop, J.L.P.; Stansbury, J.W.; Guymon, C.A. Kinetically controlled photoinduced phase separation for hybrid radical/cationic systems. *Macromolecules* **2019**, *52*, 2975–2986. [CrossRef]

26. Cook, W.D.; Chen, F.; Ooi, S.K.; Moorhoff, C.; Knott, R. Effect of curing order on the curing kinetics and morphology of bisGMA/DGEBA interpenetrating polymer networks. *Polym. Int.* **2006**, *55*, 1027–1039. [CrossRef]

27. Dean, K.; Cook, W.D.; Zipper, M.D.; Burchill, P. Curing behaviour of IPNs formed from model VERs and epoxy systems I amine cured epoxy. *Polymer* **2001**, *42*, 1345–1359. [CrossRef]

28. Jansen, B.J.P.; Rastogi, S.; Meijer, H.E.H.; Lemstra, P.J. Rubber-modified glassy amorphous polymers prepared via chemically induced phase separation. 4. Comparison of properties of semi-and full-IPNs, and copolymers of acrylate−aliphatic epoxy systems. *Macromolecules* **1999**, *32*, 6290–6297. [CrossRef]

29. Biedron, T.; Brzezinska, K.; Kubisa, P.; Penczek, S. Macromonomers by activated polymerization of oxiranes. Synthesis and polymerization. *Polym. Int.* **1995**, *36*, 73–80. [CrossRef]

30. Yagci, Y. Photoinitiated cationic polymerization of unconventional monomers. *Macromol. Symp.* **2006**, *240*, 93–101. [CrossRef]

31. Lin, J.; Wu, X.; Zheng, C.; Zhang, P.; Li, Q.; Wang, W.; Yang, Z. A novolac epoxy resin modified polyurethane acrylates polymer grafted network with enhanced thermal and mechanical properties. *J. Polym. Res.* **2014**, *21*, 435. [CrossRef]

32. Touhsaent, R.E.; Thomas, D.A.; Sperling, L.H. Epoxy/acrylic simultaneous interpenetrating networks. *J. Polym. Sci. Polym. Symp.* **1974**, *46*, 175–190. [CrossRef]

33. Scarito, P.R.; Sperling, L.H. Effect of grafting on phase volume fraction, composition, and mechanical behavior: Epoxy/poly (n-butyl acrylate) simultaneous interpenetrating networks. *Polym. Eng. Sci.* **1979**, *19*, 297–303. [CrossRef]

34. Dong, T.V.; Tinh, V.D.C.; Kim, D. Ether-free sulfonated poly (fluorene biphenyl indole) membranes and ionomer binders for proton exchange membrane fuel cells. *J. Power Sources* **2023**, *556*, 232418. [CrossRef]

35. Jeon, Y.; Tinh, V.D.C.; Thuc, V.D.; Kim, D. Ether-free polymer based bipolar electrolyte membranes without an interlayer catalyst for water electrolysis with durability at a high current density. *Chem. Eng. J.* **2023**, *459*, 141467. [CrossRef]

36. Fijten, M.W.; Paulus, R.M.; Schubert, U.S. Systematic parallel investigation of RAFT polymerizations for eight different (meth) acrylates: A basis for the designed synthesis of block and random copolymers. *J. Polym. Sci. A Polym. Chem.* **2005**, *43*, 3831–3839. [CrossRef]

37. Chiefari, J.; Chong, Y.K.; Ercole, F.; Krstina, J.; Jeffery, J.; Le, T.P.; Mayadunne, R.T.; Meijs, G.F.; Moad, C.L.; Moad, G.; et al. Living free-radical polymerization by reversible addition-fragmentation chain transfer: The RAFT process. *Macromolecules* **1998**, *31*, 5559–5562. [CrossRef]

38. Perrier, S. 50th anniversary perspective: RAFT polymerization—A user guide. *Macromolecules* **2017**, *50*, 7433–7447. [CrossRef]

39. Gu, J.; Narang, S.C.; Pearce, E.M. Curing of epoxy resins with diphenyliodonium salts as thermal initiators. *J. Appl. Polym. Sci.* **1985**, *30*, 2997–3007. [CrossRef]

40. Lu, H.; Lovell, L.G.; Bowman, C.N. Exploiting the heterogeneity of cross-linked photopolymers to create high-Tg polymers from polymerizations performed at ambient conditions. *Macromolecules* **2001**, *34*, 8021–8025. [CrossRef]

41. Anseth, K.S.; Bowman, C.N.; Peppas, N.A. Dynamic mechanical studies of the glass transition temperature of photopolymerized multifunctional acrylates. *Polym. Bull.* **1993**, *31*, 229–233. [CrossRef]

42. Poly(tetrahydrofuran). Available online: https://polymerdatabase.com/polymers/polytetrahydrofuran.html (accessed on 7 March 2023).

43. Menard, K.P. *Dynamic Mechanical Analysis: A Practical Introduction*, 2nd ed.; CRC Press: Boca Raton, FL, USA, 2008.

44. Murayama, T. *Dynamic Mechanical Analysis of Polymeric Materials*; Elsevier Scientific Publishing: New York, NY, USA, 1978.

45. Thermal Transitions of Homopolymers: Glass Transition & Melting Point. Available online: https://www.sigmaaldrich.com/US/en/technical-documents/technical-article/materials-science-and-engineering/polymer-synthesis/thermal-transitions-of-homopolymers (accessed on 7 March 2023).

46. Deane, O.J.; Jennings, J.; Neal, T.J.; Musa, O.M.; Fernyhough, A.; Armes, S.P. Synthesis and aqueous solution properties of shape-shifting stimulus-responsive diblock copolymer nano-objects. *Chem. Mat.* **2021**, *33*, 7767–7779. [CrossRef]
47. Hiemenz, P.C.; Lodge, T.P. *Polymer Chemistry*, 2nd ed.; CRC Press: New York, NY, USA, 2007; p. 494.